Journal of Power Sources 203 (2012) 121–125

Contents lists available at SciVerse ScienceDirect

Journal of Power Sources

journal homepage: www.elsevier.com/locate/jpowsour

Short communication

Porous $Li_3V_2(PO_4)_3$/C cathode with extremely high-rate capacity prepared by a sol–gel-combustion method for fast charging and discharging

Le Zhang, Hongfa Xiang, Zhong Li, Haihui Wang*

School of Chemistry & Chemical Engineering, South China University of Technology, Wushan Road, Guangzhou 510640, China

ARTICLE INFO

Article history:
Received 7 July 2011
Received in revised form
11 November 2011
Accepted 30 November 2011
Available online 8 December 2011

Keywords:
Lithium vanadium phosphate
Porous structure
Sol–gel-combustion
High rate capacity

ABSTRACT

Porous $Li_3V_2(PO_4)_3$/C (LVP/C) cathode materials have been synthesized via a sol–gel-combustion method. The porous LVP/C shows stable and extremely high rate capacity, owing to the special porous structure and the nano-sized particle. In the potential range of 3.0–4.3 V, discharge capacities of 122, 114, 108 and 88 mAh g^{-1} can be delivered at high rates of 10, 20, 40 and 60 C after 100 cycles, respectively. In the potential range of 3.0–4.8 V, the corresponding discharge capacities are 145, 129, 122, 114 and 103 mAh g^{-1} after 500 cycles at 10, 20, 40, 60 and 100 C, which is the highest level for LVP so far.

1. Introduction

The storage of electric energy is an important technology, which can enable hybrid electric vehicles (HEVs) and electric vehicles (EVs) and provide back-up for wind and solar energy [1]. Lithium ion batteries (LIBs) are considered the most efficient energy storage systems owing to their high power density and long cycle life [2–5]. As a cathode material for LIBs, monoclinic $Li_3V_2(PO_4)_3$ (LVP) is highly promising, due to its low cost, high safety and the highest theoretical capacity (197 mAh g^{-1}) among the lithium metal phosphates [6–9]. Furthermore, LVP provides good ionic conductivity because it has a three-dimensional path for lithium ion diffusion [4,10]. However, the inherent electron conductivity of LVP is poor, which leads to the poor rate performance. Different strategies are reported to improve the rate performance of LVP, such as cation doping [8,11–13], conductive material coating [14–16] and nanotechnologies [17,18]. However, the high rate performance of LVP/C which is prepared using these methods has not been significantly improved, especially in the range of 3.0–4.8 V. Thus, it is attractive to find a facile method to synthesize LVP/C with high-rate capacity.

Herein, we propose a strategy that the LVP is designed in a form of pore-containing nano-sized particles with a thin carbon layer covering all the surfaces, which combines the advantages of porous structure and carbon-coating. As illustrated in Fig. 1, the pores serve as fast channels for lithium ions and reduce the distance of lithium ion diffusion, resulting in improved ionic conductivity for LVP. Furthermore, the carbon-coating could improve the electron conductivity and prevent the aggregation of nanoparticles. Considering these two points, the special porous structure would lead to an improved electrochemical performance. To get this nano-sized LVP/C with porous structure, a novel modified sol–gel method, i.e. sol–gel-combustion method was employed. Firstly, a porous precursor is obtained during the combustion process due to the degradation of chelates or citrate anion. Then the porous precursor was mixed with the sucrose and calcined at 800 °C, the carbon, which comes from the pyrolysis of sucrose, could deposit on the wall of pores and surface of particle to form carbon coating. Compared to traditional sol–gel method [19,20], uniform carbon coating on the wall of pores can be easily achieved via the sol–gel-combustion method, which is beneficial to improve the electron conductivity and restrict the growth of particle. Thus, the nano-sized LVP/C with porous structure prepared by this method would possess high-rate performance.

2. Experimental

The porous LVP/C composites were synthesized by a sol–gel-combustion method. Firstly, 0.1125 mol citric acid monohydrate was dissolved into 100 mL deionized water. Then 0.03 mol NH_4VO_3 and 0.045 mol LiH_2PO_4 were added into citric acid solution. After stirring for a time, 0.015 mol ethylene glycol and 0.0225 mol NH_4NO_3 were added to the mixed solution. After that the solution was stirred and evaporated at 100 °C to obtain a dark blue gel. Then the gel was ignited on an electric furnace in air and burned away

* Corresponding author. Tel.: +86 20 87110131; fax: +86 20 87110131.
E-mail address: hhwang@scut.edu.cn (H. Wang).

0378-7753/$ – see front matter © 2011 Elsevier B.V. All rights reserved.
doi:10.1016/j.jpowsour.2011.11.082

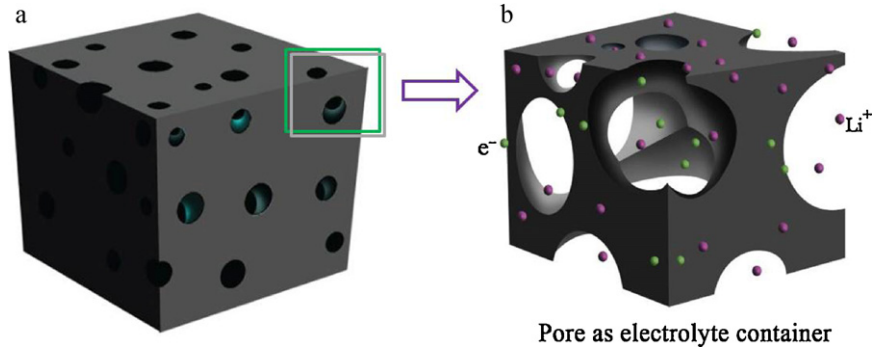

Fig. 1. Schematic illustration of the porous LVP/C composite.

for 20 min to get the brown precursor. Temperature of the furnace was 500 °C. Finally the obtained precursor was ground with 30 wt% sucrose in acetone and calcined at 800 °C for 8 h in a N_2 atmosphere to form the LVP/C composites.

The structure of the as-prepared samples was performed by X-ray diffraction (XRD, Bruker, D8 ADVANCE). The carbon content was determined by element analyzer (Vario EL III). The particle morphology was observed by transmission electron microscopy (TEM, Hitachi, JEM-2010HR). The specific surface area and the pore-size distribution were obtained by Micromeritics, ASAP2020.

The electrochemical measurements were carried out by fabricating a coin cell. A metallic lithium foil was served as the anode. The cathode electrodes were prepared by mixing LVP/C with Super P carbon and poly(vinylidene fluoride) (PVDF) at a weight ratio of 80:12:8 in *N*-methyl-2-pyrrolidinone to form a slurry. Then, the resultant slurry was uniformly pasted on Al foil with a blade, and dried at 80 °C in vacuum. The mass loading was about 1.5 mg cm^{-2} and the diameter of the electrode was 14 mm. The Celgard 2400 microporous membrane was used as a separator and the electrolyte was a solution of 1 M $LiPF_6$/ethylene carbonate + dimethyl carbonate (1:1 in volume). The coin cells were assembled in an argon-filled glove box and galvanostatically cycled in the voltage ranges of 3.0–4.3 V and 3.0–4.8 V using a Battery Testing System (Neware Electronic Co., China). In this paper, 1 C means 133 mA g^{-1} (or 0.2 mA cm^{-2}) and 197 mA g^{-1} (or 0.3 mA cm^{-2}) in the voltage ranges of 3.0–4.3 V and 3.0–4.8 V, respectively. The discharge rate was the same as the charge rate during every cycle.

3. Results and discussion

Fig. 2(a) shows the XRD patterns of the precursor and the LVP/C composite. It is found that the precursor is completely amorphous and the LVP/C composite presents a well-crystallized monoclinic phase with the space group of $P2_1/n$ although there is a small

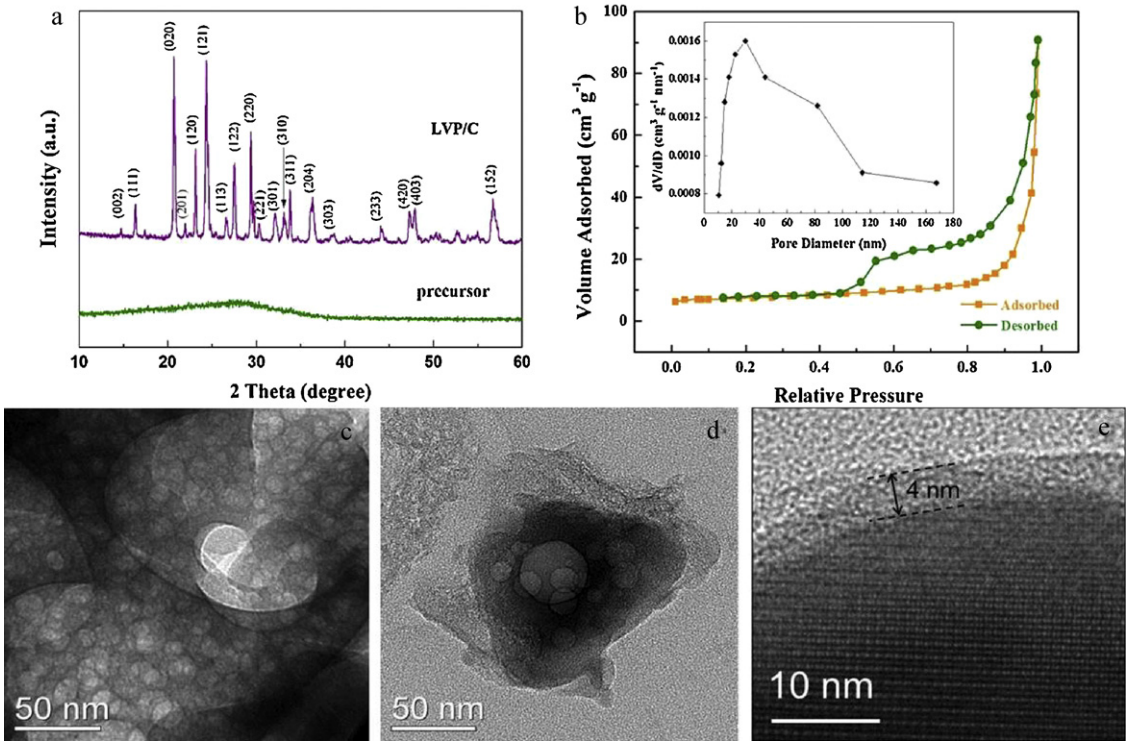

Fig. 2. (a) XRD patterns of the precursor and the LVP/C composite; (b) N_2 adsorption/desorption isotherm, the pore-size distribution curve corresponding BJH (inset); (c) TEM image of the precursor; (d and e) TEM images of LVP/C.

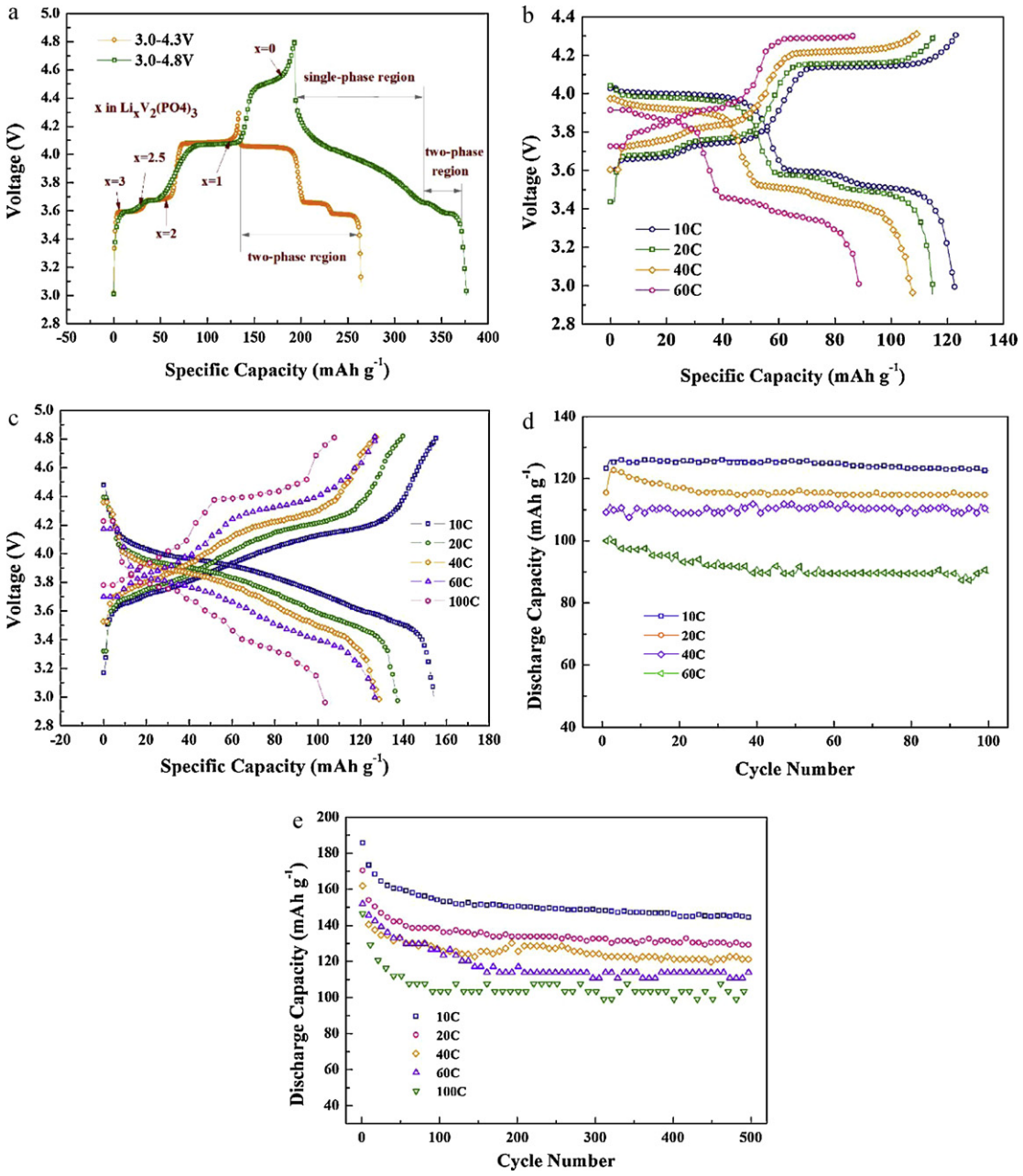

Fig. 3. (a) Initial charge/discharge curves at 0.2 C in the voltage range of 3.0–4.3 V (1 C = 133 mA g^{-1} or 0.2 mA cm^{-2}) and 3.0–4.8 V (1 C = 197 mA g^{-1} or 0.3 mA cm^{-2}); (b) the 100th charge/discharge curves at different rates between 3.0 and 4.3 V; (c) the 100th charge/discharge curves at different rates between 3.0 and 4.8 V; (d) cycling performance at the rate from 10 to 60 C between 3.0 and 4.3 V; (e) cycling performance from 10 to 100 C between 3.0 and 4.8 V.

unidentified peak at 2θ of 18. The similar results have been reported in the literatures [21–24]. These impurities would not affect the performance of final product, which is also found in the literatures mentioned above. Moreover, no carbon phase is detected in the LVP/C composite, indicating that carbon generated from sucrose is amorphous and its presence does not influence the crystal structure of LVP. According to the element analysis results, the carbon contents of precursor and final product are 0.1 wt% and 5.4 wt%, respectively.

As shown in Fig. 2(c), the precursor exhibits a novel spongy-shaped porous network structure, and the diameter of the pores is about 20–30 nm. When the porous precursor mixed with the sucrose is calcined at 800 °C, the carbon, which comes from the pyrolysis of sucrose, could deposit on the wall of pores and surface of particle to form carbon coating. Compared to traditional sol–gel method, uniform carbon coating on the wall of pores can be easily achieved via the sol–gel-combustion method, which helps to improve the electron conductivity and restrict the growth of particle. In Fig. 2(d), the porous structure of a LVP particle is visible. The diameter of LVP particles and the pores is about 100–150 nm and 10–25 nm, respectively. The HR-TEM image of the final product is shown in Fig. 2(e). It is found that the thickness of the carbon coating is about 4 nm. In order to further investigate the porous structure, N_2 adsorption/desorption isotherms are measured. The Brunauer–Emmett–Teller (BET) specific surface area is 25.7 m^2 g^{-1} and the Barrett–Joyner–Halenda (BJH) pore-size distribution indicates that the sample contains broadly distributed pores with sizes below 40 nm, as shown in Fig. 2(b). When filled with liquid

electrolyte, the existence of the pores could reduce the distance of ion diffusion and increase the contact area between electrode and electrolyte. The porous structure and the carbon coating are responsible for easy ion exchange and good electron conductivity, respectively. Thus, an excellent rate performance can be expected even at super high current densities [19].

It is reported that the mechanism of monoclinic LVP charging and discharging is complex [25–27]. The charge/discharge curves of LVP/C composite at 0.2 C are shown in Fig. 3(a) to analyze the charge/discharge process. When LVP is charged up to 4.3 V, two Li^+ will be extracted from LVP. There are three plateaus around 3.59, 3.67 and 4.08 V, corresponding to a series of phase transition processes: $Li_3V_2(PO_4)_3 \rightarrow Li_{2.5}V_2(PO_4)_3 \rightarrow Li_2V_2(PO_4)_3 \rightarrow LiV_2(PO_4)_3$ [13]. During the process, the first Li^+ is extracted in two steps because of the existence of an ordered phase $Li_{2.5}V_2(PO_4)_3$. In the discharge process, the two Li^+ can reversibly insert into $LiV_2(PO_4)_3$. When charged up to 4.8 V, the extraction of the third Li^+ will take place corresponding to the fourth plateaus around 4.52 V, which is the most difficult due to the low ionic and electronic conductivity of the $V_2(PO_4)_3$. In the discharge process, a solid solution behavior (i.e. single-phase region) is initially displayed as indicated by the characteristic S-shaped curve [3]. Subsequently, there are two electrochemical plateaus on the curve which exhibit its two-phase transition behavior, $Li_2V_2(PO_4)_3 \rightarrow Li_{2.5}V_2(PO_4)_3 \rightarrow Li_3V_2(PO_4)_3$, corresponding to the reinsertion of the last Li^+.

The rate capability and the cycling performance of LVP/C composite are investigated, as shown in Fig. 3(b)–(e). A high discharge capacity of 122 mAh g^{-1} is delivered (about 92.0% of the theoretical capacity) at the rate of 10 C after 100 cycles in the range of 3.0–4.3 V (Fig. 3(b)). The specific capacity gradually decreases with increasing current rate. The discharge capacities are 114, 108 and 88 mAh g^{-1} at high rates of 20, 40 and 60 C after 100 cycles, respectively. The coulombic efficiency of the composite is close to 100%, indicating good electrochemical reversibility. It could also be found that the plateaus become shorter and the differences of the charge and discharge plateaus become larger gradually with the rate increase. The reason for this phenomenon may be the electrode polarization at high rates [22]. The 100th charge/discharge curves between 3.0 and 4.8 V are shown in Fig. 3(c). The discharge capacities of 154, 137, 129 and 126 mAh g^{-1} are delivered at 10, 20, 40, 60 C after 100 cycles, respectively. At an extremely high rate of 100 C, a capacity of 104 mAh g^{-1} is still delivered. As far as we know, such a good rate performance of the LVP/C composite has never been reported before. Fig. 3(d) presents cycling performance of LVP between 3.0 and 4.3 V at 10, 20, 40 and 60 C. At the charge/discharge window of 3.0–4.3 V, the initial capacities are 123, 116, 109 and 100 mAh g^{-1} at 10, 20, 40 and 60 C. After 100 cycles, the capacities become 122, 114, 108 and 88 mAh g^{-1}, respectively. The capacity retentions are 99.2–88.0% % from 10 to 60 C. At the charge/discharge window of 3.0–4.8 V, the initial capacities are 184, 170, 162, 154 and 146 mAh g^{-1} at 10, 20, 40, 60 and 100 C, respectively, as shown in Fig. 3(e). During the first dozens of cycles the capacity of the LVP/C decreases rapidly. Then, the discharge capacity gradually stabilizes. After 100 cycles the capacity retentions are 83.7%–71.2% from 10 to 100 C at the charge/discharge window of 3.0–4.8 V, which are lower than that at the charge/discharge window of 3.0–4.3 V. After a long-term cycling of 500 times, capacities of 145, 129, 122, 114 and 103 mAh g^{-1} can be delivered at the rates of 10, 20, 40, 60 and 100 C, respectively. The capacity loss in this voltage range is often reported by other researchers [3,25], which may be caused by the electrolyte decomposition and the increasing impedance at high voltage [10,28].

A specific capacity of 80 mAh g^{-1} at 24 C (1 C means 118 mA g^{-1} or 0.19 mA cm^{-2}) rate was achieved by Wang et al. [2] in the potential range of 3.0–4.3 V for the thin-film LVP/C composite, which was prepared by a complex method named electrostatic spray deposition (ESD). Recently, Pan et al. [4] prepared LVP/C composite with the help of a special mesopores carbon. They obtained the capacity of 83 mAh g^{-1} in 3.0–4.3 V at 32 C rate (1 C means 140 mA g^{-1} or 0.21 mA cm^{-2}). In the present work, the specific capacities of LVP/C are 86 mAh g^{-1} at 60 C rate between 3.0 and 4.3 V and 105 mAh g^{-1} at 100 C rate between 3.0 and 4.8 V, respectively. The main reasons for the excellent rate performance are the special porous structure with carbon-coating on the surface and the nano-sized particle. Furthermore, the sol–gel-combustion method is a simple way to synthesize the porous LVP/C composite with the extremely high-rate capacity.

4. Conclusion

Porous LVP/C cathode materials are synthesized via a sol–gel-combustion method and present extremely excellent high-rate performance. The as-prepared porous LVP/C exhibits an excellent specific capacity of 105 mAh g^{-1} at 100 C rate between 3.0 and 4.8 V. This performance enhancement is attributed to the porous structure with a thin carbon layer covering all the surfaces and the nano-sized particle, which could improve the ion diffusion and electron conductivity. The materials synthesized in this paper are promising to be used for fast charging and discharging and the sol–gel-combustion method is a simple and universal way to prepare the high performance materials.

Acknowledgments

This work was supported by National Science Foundation of China (grant no. 21006033), Program for New Century Excellent Talents in Chinese Ministry of Education (no. NECT-07-0307) and the Fundamental Research Funds for the Central Universities, SCUT (2009220038).

References

[1] B. Kang, G. Ceder, Nature 458 (2009) 190–193.
[2] L. Wang, L.C. Zhang, L. Lieberwirth, H.W. Xu, C.H. Chen, Electrochem. Commun. 12 (2010) 52–55.
[3] X.H. Rui, C. Li, J. Liu, T. Cheng, C.H. Chen, Electrochim. Acta 55 (2010) 6761–6767.
[4] A.Q. Pan, J. Liu, J.G. Zhang, W. Xu, G.Z. Cao, Z.M. Nie, B.W. Arey, S.Q. Liang, Electrochem. Commun. 12 (2010) 1674–1677.
[5] M.M. Ren, Z. Zhou, Y.Z. Li, X.P. Gao, J. Yan, J. Power Sources 162 (2006) 1357–1362.
[6] M.Y. Saidi, J. Barker, H. Huang, J.L. Sowyer, G. Adamson, J. Power Sources 119–121 (2003) 266–272.
[7] W.F. Howard, R.M. Spotnitz, J. Power Sources 165 (2007) 887–891.
[8] P. Fu, Y.M. Zhao, Y.Z. Dong, X.N. An, G.P. Shen, J. Power Sources 162 (2006) 651–657.
[9] M. Sato, H. Ohkawa, K. Yoshida, M. Saito, K. Uematsu, K. Toda, Solid State Ionics 135 (2000) 137–142.
[10] S. Patoux, C. Wurm, M. Morcrette, G. Rousse, C. Masquelier, J. Power Sources 119 (2003) 278–284.
[11] C.S. Dai, Z.Y. Chen, H.Z. Jin, X.G. Hu, J. Power Sources 195 (2010) 5775–5779.
[12] J. Barker, R.K.B. Gover, P. Burns, A. Bryan, J. Electrochem. Soc. 154 (2007) A307–A313.
[13] Q. Kuang, Y.M. Zhao, X.N. An, J.M. Liu, Y.Z. Dong, L. Chen, Electrochim. Acta 55 (2010) 1575–1581.
[14] M.M. Ren, Z. Zhou, X.P. Gao, W.X. Peng, J.P. Wei, J. Phys. Chem. C 112 (2008) 5689–5693.
[15] C.X. Chang, J.F. Xiang, X.X. Shi, X.Y. Han, L.J. Yuan, J.T. Sun, Electrochim. Acta 54 (2008) 623–627.
[16] L. Zhang, X.L. Wang, J.Y. Xiang, Y. Zhou, S.J. Shi, J.P. Tu, J. Power Sources 195 (2010) 5057–5061.
[17] A.Q. Pan, D.W. Choi, J.G. Zhang, S.Q. Liang, G.Z. Cao, Z.M. Nie, B.W. Arey, J. Liu, J. Power Sources 196 (2011) 3646–3649.
[18] A.Q. Pan, J.G. Zhang, Z.M. Nie, G.Z. Cao, B.W. Arey, G. Li, S.Q. Liang, J. Liu, J. Mater. Chem. 20 (2010) 9193–9199.
[19] R. Dominko, M. Bele, M. Gaberscek, M. Remskar, D. Hanzel, J.M. Goupil, S. Pejovnik, J. Jamnik, J. Power Sources 153 (2006) 274–280.
[20] Y.K. Zhou, J. Wang, Y.Y. Hu, R. O'Hayre, Z.P. Shao, Chem. Commun. 46 (2010) 7151–7153.

[21] J.C. Zheng, X.H. Li, Z.X. Wang, H.J. Guo, Q.Y. Hu, W.J. Peng, J. Power Sources 189 (2009) 476–479.
[22] Y.Q. Qiao, J.P. Tu, X.L. Wang, D. Zhang, J.Y. Xiang, Y.J. Mai, C.D. Gu, J. Power Sources 196 (2011) 7715–7720.
[23] B. Huang, X.P. Fan, X.D. Zheng, M. Lu, J. Alloys Compd. 509 (2011) 4765–4768.
[24] G. Yang, H.D. Liu, H.M. Ji, Z.Z. Chen, X.F. Jiang, Electrochim. Acta 55 (2010) 2951–2957.
[25] L.J. Wang, X.C. Zhou, Y.L. Guo, J. Power Sources 195 (2010) 2844–2850.
[26] S.C. Yin, H. Grondey, P. Strobel, M. Anne, L.F. Nazar, J. Am. Chem. Soc. 125 (2003) 10402–10411.
[27] H.D. Liu, P. Gao, J.H. Fang, G. Yang, Chem. Commun. 47 (2011) 9110–9112.
[28] X.H. Rui, C. Li, C.H. Chen, Electrochim. Acta 54 (2009) 3374–3380.